The Chemistry of the Thiosulfinyl Group: Preparation, Structure, and Spectroscopic and Chemical Properties of Cyclic Thionosulfites

by **Juzo Nakayama***, **Sanae Yoshida (nee Tanaka)**, **Yoshiaki Sugihara**, and **Akira Sakamoto**

Department of Chemistry, Faculty of Science, Saitama University, Sakura-ku, Saitama, Saitama 338-8570, Japan (phone and fax: +81 48-858-3390; e-mail: nakaj@post.saitama-u.ac.jp)

Dedicated to Professor *Rolf Huisgen* on the occasion of his 85th birthday

Treatment of the tetrahydrothiophene-3,4-diol **5** with 1,1′-thiobis-(1*H*-benzimidazole) (**6**) furnished two diastereoisomers of the novel cyclic thionosulfite **4** with different configurations at the pseudo-tetrahedral center of the thiosulfinyl (S=S) group. The configuration of the S=S group of the major diastereoisomer (isolated in 45% yield) was established to be *syn* to the thiolane ring, as determined by X-ray crystallographic analysis, while that of the minor diastereoisomer (isolated in 10% yield) was *anti*. ^{1}H-NMR Spectroscopic analysis clarified that the shielding and deshielding zones of the S=S group are similar to those of the well-documented S=O group. Characteristic absorptions of the S=S group in the IR, *Raman*, and UV/VIS spectra were assigned on the basis of calculations at the B3LYP/6-31G* level. The reactivity of the S=S group toward thermolysis, hydrolysis, and oxidation was examined. The S=S group is more resistant toward oxidation than the divalent sulfide S-atom, but is oxidatively converted to the S=O group.

1. Introduction. – Much effort has been devoted to developing the chemistry of the thiosulfinyl group, a highly reactive functional group, but much still remains to be explored[1]). $F_2S{=}S$ (**1**) is a long-known compound. Its S=S bond length was determined to be 1.860 Å by microwave spectroscopy in 1963 [2]. The first synthesis of thionosulfites $(RO)_2S{=}S$ was reported in 1965 [3a]. In this report, the isomeric dialkoxy disulfide structure ROSSOR was ruled out on the basis of ^{1}H-NMR analysis of cyclic derivatives. Later, a more-stable thionosulfite, **2**, was synthesized, and its molecular structure was determined by X-ray single-crystal structure analysis by *Harpp et al.* [4a,c]. The S=S bond length (1.901 Å) of **2** is clearly shorter than those of common disulfides (2.03–2.07 Å) [5], and is of the same order as that of **1** (1.860 Å), diatomic sulfur $^{134}S_2$ (1.890 Å) [6], and *N*-(thiosulfinyl)amines (−N=S=S) (1.898, 1.918 Å) [7]. On the other hand, although thiosulfoxides (R = alkyl or aryl for $R_2S{=}S$) have been proposed occasionally as transient intermediates, they still elude detection even by spectroscopic methods [1]. This suggests that the thiosulfinyl group is more stabilized by heteroatom substituents such as F and RO than by alkyl or aryl groups [3].

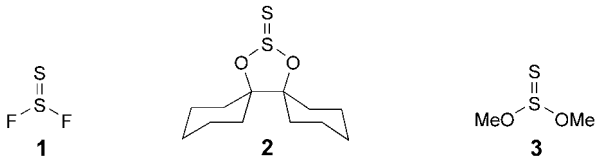

[1]) For a leading review, see [1].

The S-atom in sulfites acts as a stereogenic center because of the stable pseudo-tetrahedral geometry. Thus, enantiomerically pure sulfites have been prepared and applied to asymmetric synthesis [8]. In this connection, the structure and reactions of thionosulfites are also of much interest. Recently, the inversion energy at the sulfur center of **3** was predicted to be 32.3 kcal/mol by calculations at the MP2/6311G(3d) level [4b]. However, reactions of the thiosulfinyl group of thionosulfites have been scarcely studied.

Herein, we report the preparation of the five-membered cyclic thionosulfite **4** by treatment of *cis*-3,4-di-(*tert*-butyl)tetrahydrothiophene-3,4-diol (**5**) [9] with 1,1′-thiobis(1*H*-benzimidazole) (**6**) [10], and the isolation of the two diastereoisomers **4a** and **4b** (see *Scheme 1* below)[2]). The structures of **4a** and **4b** are discussed on the basis of X-ray crystallographic analyses, spectral data, and density functional theory (DFT) calculations. Also reported are the diamagnetic anisotropy and chemical properties of the S=S group.

2. Results and Discussion. – 2.1. *Preparation of Thionosulfites* **4a** *and* **4b**. Initially, we thought that **4** could be derived from the corresponding sulfite **7** by replacement of its O-atom by an S-atom. Thus, **7** was prepared by condensation of **5** [9] with $SOCl_2$ as a mixture of the diastereoisomers **7a** and **7b** [12][13]. Disappointingly, however, the attempted conversion of **7** to **4** by treatment with *Lawesson*'s reagent was unsuccessful (*Scheme 1*).

Previously, *Harpp et al.* showed that thionosulfites are produced from 1,2-diols by treatment with **6** [10]. We applied this method to **5** to obtain **4** directly [4a] (*Scheme 1*). Thus, the reaction of **5** with **6** was studied by varying the solvent, the amount of **6**, the temperature, and the reaction time. As a result, it was found that the yield of **4** was optimal when **5** was treated with 4 mol-equiv. of **6** in MeCN for 72 h at room temperature. Under these conditions, the reaction led to a mixture of the diastereoisomers **4a** and **4b** in a ratio of 82:18. Separation by HPLC afforded **4a** and **4b** in 45% and 10% yield, respectively. Similar results were obtained when the reaction was conducted at 40° for 48 h. When 4 mol-equiv. of 1,2,4-triazole were used as an additive, the yield of **4** slightly increased to afford **4a** and **4b** in 50% and 11% yield, respectively. However, we cannot explain how the additive improves the yield. Pretreatment of **5** with a base such as *t*-BuOK or BuLi in THF and subsequent treatment with **6** gave rise to byproducts, with formation of **4** in decreased yield.

The use of 1,1′-thiobis(1*H*-1,2,4-triazole) (**8**) [10] instead of **6** gave **4** in low yield (14% for **4a**, and 6% for **4b**). Although the use of 1,1′-dithiobis(1*H*-benzimidazole) (**9**) [10] gave a small amount of **4**, its formation might be due to the presence of **6** as a contaminant. The use of sulfur dichloride (SCl_2) or sulfur monochloride (S_2Cl_2) did not afford **4** even in trace amounts.

A probable mechanism for the formation of **4** is shown in *Scheme 2*. The initial reaction would involve a sulfur transfer from **6** to **5** to produce the dioxathiolane **10**, with elimination of two molecules of benzimidazole. The S-atom of **10**, which is activated by repulsive lone-pair–lone-pair interactions with the adjacent O-atoms,

---

[2]) Part of this work was preliminarily reported [11].

Scheme 1

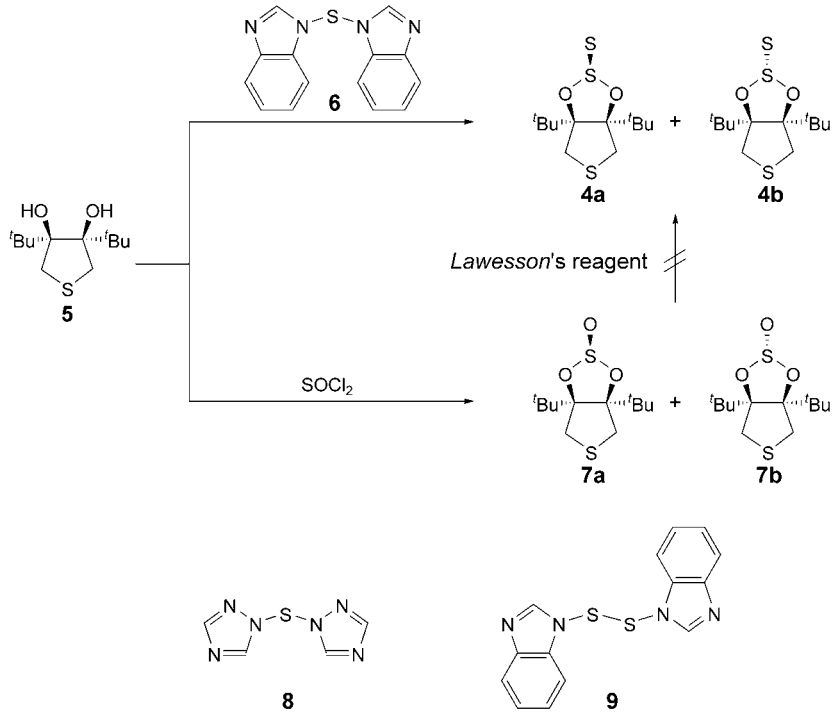

Scheme 2

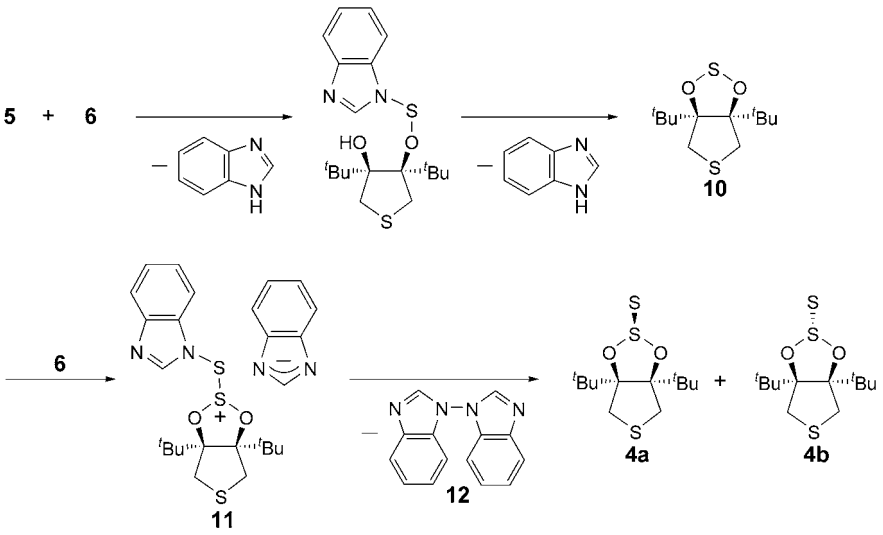

would further react with **6** to give the ionic intermediate **11**. Finally, the elimination of 1,1′-bi-1*H*-benzimidazole (**12**) [14] from **11** leads to the formation of **4a** and **4b**.

2.2. *Molecular Structures of* **4a** *and* **4b**. The configuration of **4a** and **4b** was established by X-ray crystallographic analysis (*Fig. 1*; for crystal data, see *Table 3* in the *Exper. Part*). *Table 1* shows the relevant bond angles, bond lengths, and dihedral angles of **4a** and **4b**, and also those of **4a** and **4b** obtained by DFT calculations (B3LYP/6-31G* level)[3]). The optimized molecular structures of **4a** and **4b** were in good agreement with the experimental structures, as is evident from *Figs. 1* and *2* (see also *Table 1*) [15].

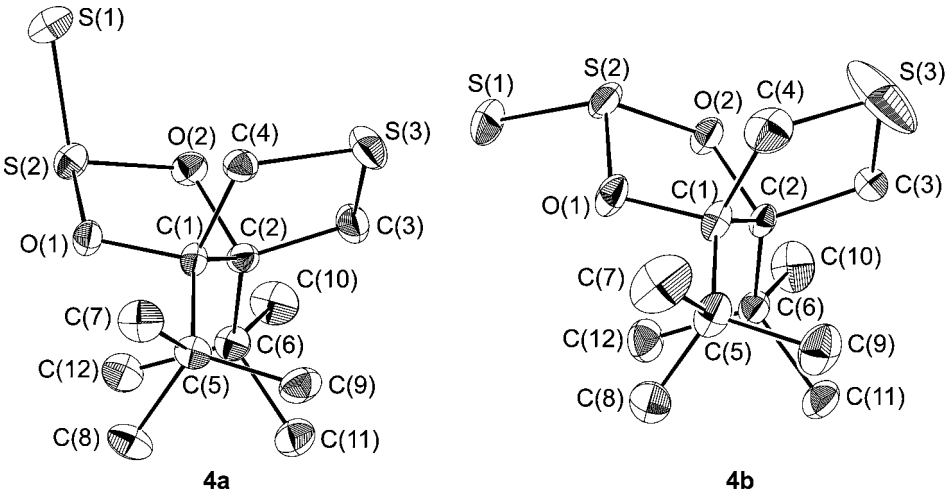

Fig. 1. *ORTEP Representations of the molecular structures of* **4a** *and* **4b**

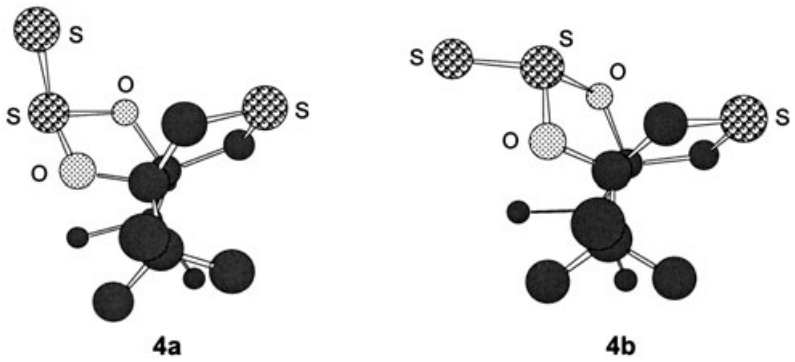

Fig. 2. *Optimized structures of* **4a** *and* **4b** *calculated at the B3LYP/6-31G* level*

[3]) The calculations were performed with the Gaussian 98 (revision A.7) program on personal computers running *RedHat Linux 6.0*. All of the geometry optimization, vibrational-frequency calculations, and time-dependent DFT calculations were carried out at the B3LYP/6-31G* level. The calculated frequencies are scaled by 0.9613.

Table 1. *Observed and Calculated* (B3LYP/6-31G*) *Bond Lengths* [Å], *Bond Angles* [°], *and Dihedral Angles* [°] *of Compounds* **4**

	Observed		Calculated	
	4a	**4b**	**4a**	**4b**
S(1)–S(2)	1.9154(6)	1.8964(13)	1.936	1.929
S(2)–O(1)	1.6399(12)	1.639(2)	1.706	1.714
S(2)–O(2)	1.6432(12)	1.644(2)	1.704	1.708
S(3)–C(3)	1.802(2)	1.750(2)	1.836	1.825
S(3)–C(4)	1.800(2)	1.787(4)	1.827	1.833
O(1)–C(1)	1.464(2)	1.475(3)	1.454	1.470
O(2)–C(2)	1.484(2)	1.457(3)	1.472	1.446
C(1)–C(2)	1.598(2)	1.607(4)	1.617	1.625
C(1)–C(4)	1.557(2)	1.527(4)	1.566	1.541
C(1)–C(5)	1.564(2)	1.574(4)	1.587	1.595
C(1)–C(3)	1.527(2)	1.556(5)	1.541	1.573
C(2)–C(6)	1.572(2)	1.575(5)	1.595	1.588
C(5)–C(7)	1.546(2)	1.545(5)	1.557	1.556
C(5)–C(8)	1.535(3)	1.540(5)	1.546	1.548
C(5)–C(9)	1.527(2)	1.530(6	1.542	1.543
C(1)–C(10)	1.541(3)	1.538(6)	1.555	1.558
C(6)–C(11)	1.534(3)	1.530(6)	1.547	1.545
C(6)–C(12)	1.534(3)	1.526(6)	1.547	1.543
S(1)–S(2)–O(1)	111.88(5)	111.69(10)	113.1	113.9
S(1)–S(2)–O(2)	106.28(5)	105.92(9)	107.0	107.2
O(1)–S(2)–O(2)	93.43(6)	92.74(11)	91.3	90.9
C(3)–S(3)–C(4)	94.25(8)	95.3(2)	92.9	93.5
S(2)–O(1)–C(1)	112.83(10)	116.1(2)	112.0	116.1
S(2)–O(2)–C(2)	113.60(9)	109.4(2)	114.0	109.7
O(1)–C(1)–C(2)	103.13(12)	100.6(2)	104.1	100.3
O(1)–C(1)–C(4)	107.82(12)	105.2(2)	108.3	104.6
C(2)–C(1)–C(4)	103.73(12)	107.7(2)	103.3	108.5
O(2)–C(2)–C(1)	98.59(11)	102.8(2)	99.2	103.8
O(2)–C(2)–C(3)	104.09(13)	108.4(3)	103.8	108.3
C(1)–C(2)–C(3)	101.82(13)	105.0(2)	108.8	104.2
S(3)–C(3)–C(2)	109.82(11)	112.3(3)	110.4	111.1
S(3)–C(4)–C(1)	109.84(11)	109.1(2)	109.0	110.6
S(1)–S(2)–O(1)–C(1)	98.37(10)	115.8(2)	98.5	111.6
S(1)–S(2)–O(2)–C(2)	132.94(10)	145.8(2)	133.8	144.8
O(1)–S(2)–O(2)–C(2)	18.99(10)	32.3(2)	19.1	29.5
O(2)–S(2)–O(1)–C(1)	10.65(10)	7.4(2)	10.7	2.3
O(1)–C(1)–C(2)–O(2)	41.86(11)	36.4(2)	42.6	40.0
C(3)–C(2)–C(1)–C(4)	37.66(14)	33.0(3)	37.6	36.1
C(5)–C(1)–C(2)–C(6)	43.7(2)	38.0(3)	43.1	41.2

For comparison, the bond angles and bond lengths around the S=S group of **4a**, and those around the S=O group of **7a** are shown in *Fig. 3* [13]. The sum of the two O–S–S bond angles and the O–S–O bond angle of **4a** is 311.5°, which is comparable with that of **7a** (309.5°), while it is smaller than the sum of three H–C–H bond angles of methane (328.5°). Incidentally, the sum of the corresponding angles is 310.4° for **4b**. The S=S bond lengths of **4a** and **4b** are 1.9154(6) and 1.8964(13) Å, respectively, and

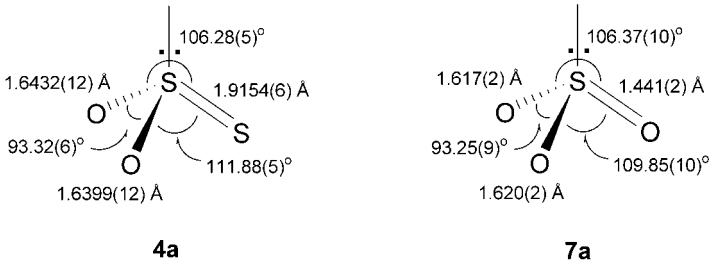

Fig. 3. *Bond angles and bond lengths around the S=S group of* **4a** *and the S=O group of* **7a**

are comparable with that of **2** (1.901(2) Å). The two *t*-Bu groups of **4a** and **4b** are twisted, with dihedral angles of 43.7(2) and 38.0(3)°, respectively, to reduce steric repulsion.

2.3. *Spectroscopy of* **4a** *and* **4b**. As to the diamagnetic anisotropy of the S=S group, no information has been available to date. *Fig. 4* shows the ^{1}H-NMR chemical-shift data of the CH_2 groups of **4a** and **4b**, and those of **7a** and **7b**. Each H-atom of these compounds appeared as a *doublet*, with $J = 13$ to 14 Hz due to geminal coupling [13]. The ^{1}H-NMR spectrum of **4a** shows two *doublets* ($J = 13.4$ Hz) at δ(H) 3.41 and 3.90, and that of **4b** shows two *doublets* ($J = 14.1$ Hz) at 3.13 and 3.42. For **4a**, the *doublet* at δ(H) 3.41 is assigned to H_b due to the observation of an 8% NOE on irradiation of the *t*-Bu H-atoms, while, for **4b**, the *doublet* at δ(H) 3.42 is assigned to H_b (13% NOE; H_b of **4a** and **4b** are *cis* to the bulky *t*-Bu groups). Thus, H_a of **4a** appears at a lower field than does H_b, while H_a of **4b** appears at higher field than H_b, similar to **7a** and **7b**.

The analysis of these data leads to the conclusion that the shielding and deshielding zones of the S=S group are similar to those of the S=O group. The shielding and deshielding zones of the S=S group are, therefore, assigned as depicted in *Fig. 5* by analogy of the corresponding well-documented zones of the S=O group [16].

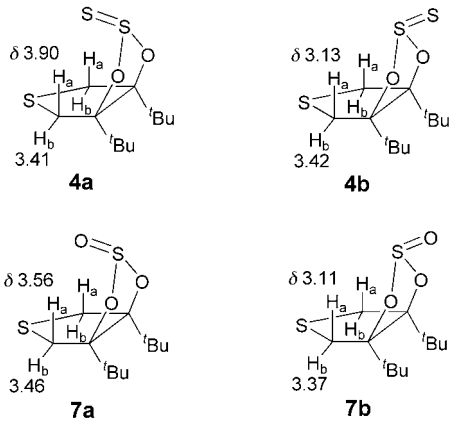

Fig. 4. *^{1}H-NMR Chemical shifts of* **4a**,**b** *and* **7a**,**b**

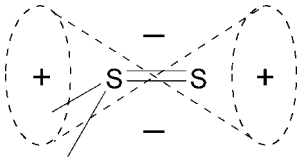

Fig. 5. *Magnetic-Shielding* (+) *and -deshielding* (–) *zones of the S=S group*

The S=S bond-stretching vibration would be the greatest concern in the IR and *Raman* spectra of **4a** and **4b**. The observed and DFT-calculated[3]) IR and *Raman* spectra of **4a** are shown in *Figs. 6* and *7*, respectively, and those of **4b** are given in *Figs. 8* and *9*, respectively [15]. Both types of spectra of **4a** showed a strong absorption band at 653 and 650 cm^{-1}, respectively. The calculations on **4a** predicted that the strong IR absorption band and the medium-sized *Raman* band appear at 639 cm^{-1}, with a scaling factor of 0.9613 mainly due to the contribution of the S=S stretching vibration. Therefore, the above-mentioned strong IR and *Raman* bands at 653 and 650 cm^{-1}, respectively, can be assigned to the S=S stretching vibration. Similarly, the strong *Raman* band assignable to the S=S stretching vibration was observed at 666 cm^{-1} for **4b**. The corresponding IR absorption band was observed at 665 cm^{-1} as a shoulder of the strong 670-cm^{-1} band. The DFT calculations of **4b** predicted the medium-sized IR

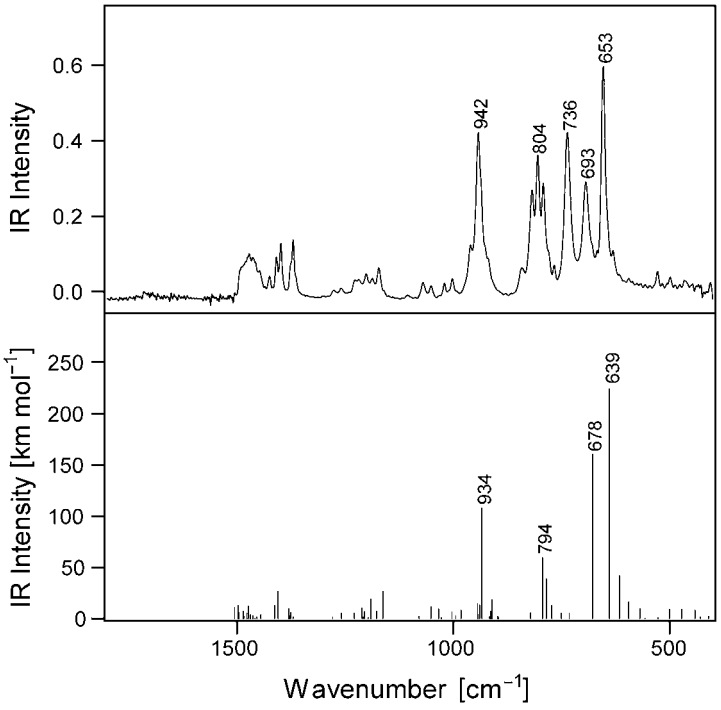

Fig. 6. *Observed* (top) vs. *calculated* (bottom) *IR spectra of* **4a**

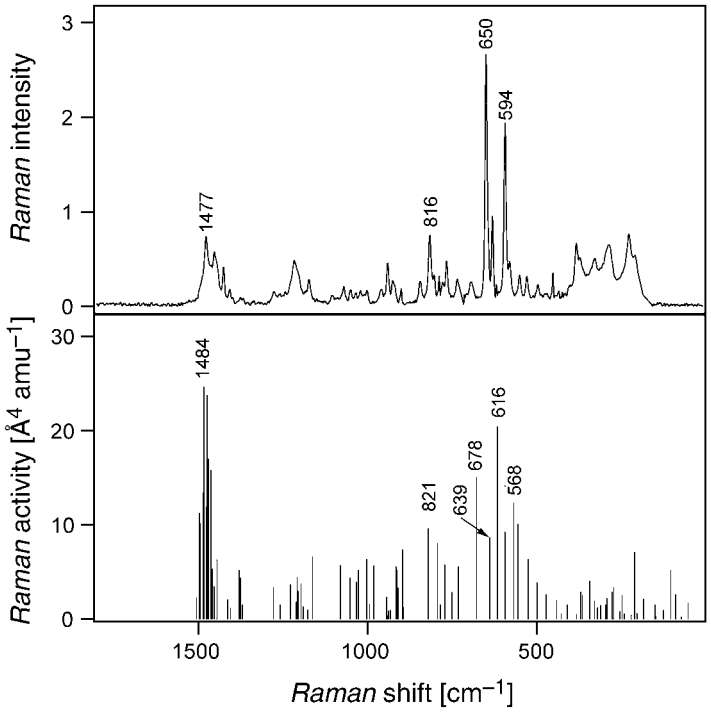

Fig. 7. *Observed* (top) vs. *calculated* (bottom) Raman *spectra of* **4a**

absorption band and the strong *Raman* band at 647 cm^{-1}, which are assignable to the S=S stretching vibration. For **2**, the S=S stretching IR and *Raman* bands are observed at 650 and 652 cm^{-1}, respectively [4b].

The UV/VIS spectrum of **4a** is shown in *Fig. 10*. Thus, **4a** showed the two absorption maxima at 253 ($\varepsilon = 2790$) and 324 (142) nm, whereas time-dependent DFT calculations predicted the appearance of two strong absorptions at 249 and 263 nm, and a weak absorption at 361 nm that originate from the S=S group. This might be rationalized by the overlap of the two expected absorptions at 249 and 263 nm, which became a single absorption at 253 nm. Similarly, **4b** showed the two absorption maxima at 245 ($\varepsilon =$ 3060) and 313 (203) nm, although the calculations predicted the appearance of the two strong absorptions at 241 and 262 nm, and the weak absorption at 351 nm. Also, for **2**, only two absorptions, a strong one at 250 nm, and a weak one at 311 nm, were observed [4b].

2.4. *Reactions of* **4a** *and* **4b**: *Thermolysis, Hydrolysis, and Oxidation*. No thermal isomerization was observed between **4a** and **4b**, even when each isomer was heated at 120° in [D_8] toluene, though some decomposition took place (*Scheme 3*). Thus, when **4a** was heated at 120° for 96 h, **13**, **14** [9], and **4a** were present in a ratio of 39 : 13 : 48. On the other hand, **4b** decomposed completely to produce **13** and **14** in a ratio of 6 : 94, when heated to 120° for 24 h. The progress of the decomposition of **4b** was monitored

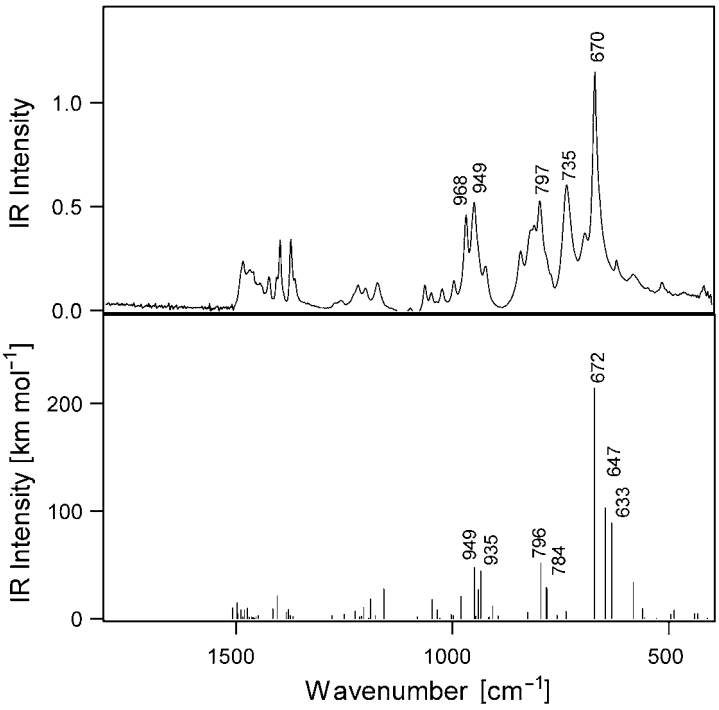

Fig. 8. *Observed* (top) vs. *calculated* (bottom) *IR spectra of* **4b**

Scheme 3

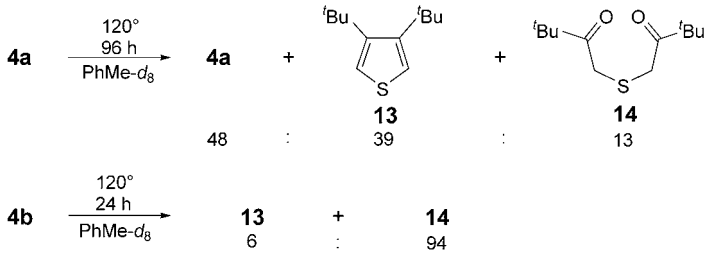

by ^{1}H-NMR analysis. Thus, we concluded that the pseudo-tetrahedral geometry around the thiosulfinyl group is rigid enough to induce a stereogenic center [4b]. Hence, the observed product ratio **4a**/**4b** of 82 : 18 is kinetically controlled.

Compounds **13** and **14** would be produced through two independent competitive pathways (*Scheme 4*). For **4a**, the terminal S-atom and one of the CH_2 H-atoms can come close together, thus enabling an intramolecular H-atom abstraction, which gives rise to the thiosulfurous acid ester **15**. Then, another intramolecular H-shift takes place in **15** to form **13** as the major product, with elimination of HOS(O)SH ($H_2S + SO_2$). Meanwhile, thermal extrusion of diatomic sulfur (S_2) of **4a** would result in the formation of **14**, with simultaneous C–C bond cleavage. The formation of **14** through

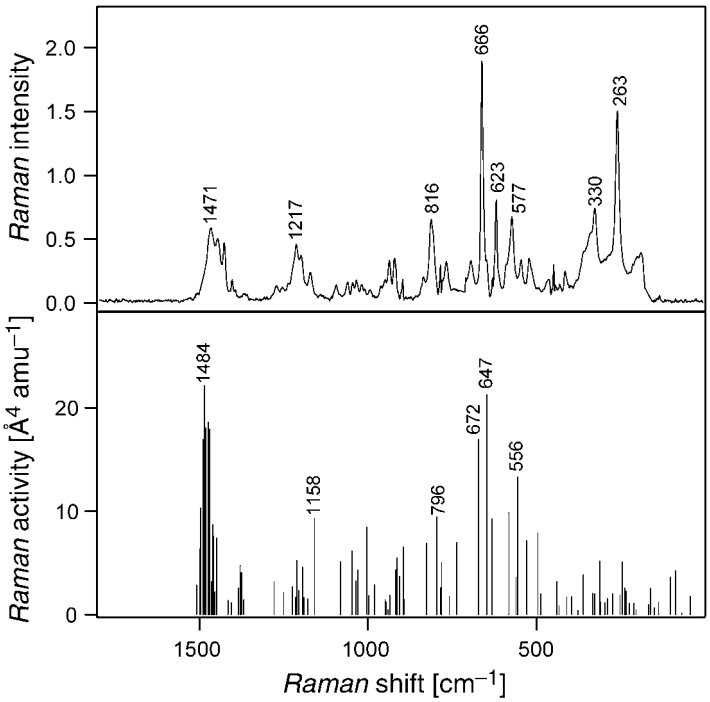

Fig. 9. *Observed* (top) vs. *calculated* (bottom) Raman *spectra of* **4b**

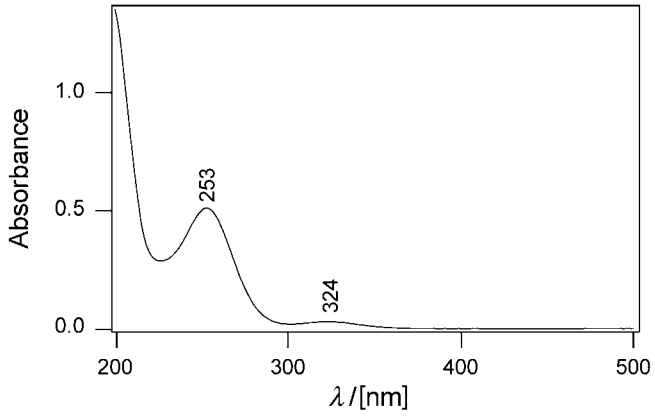

Fig. 10. *UV/VIS Spectrum of* **4a**

the dioxetane intermediate **16**, which is formed by loss of S_2, would be disfavorable. On the other hand, for **4b**, the foregoing intramolecular H-shift is difficult to occur, because the terminal S-atom is remote from the CH_2 H-atoms. Therefore, the decomposition of **4b** would take place predominantly with liberation of S_2 to give **14** as the major product. The minor product **13** from **4b** might be rationalized as intermolecular H-atom

abstraction, by which two molecules of **4b** produce two molecules of **15**. The formation of **13**, through isomerization of **4b** to **4a** by pyramidal inversion followed by intramolecular H-atom abstraction, would be least probable, because **4a** is thermally more stable than **4b**. The DFT calculations also predicted that **4a** is thermodynamically more stable than **4b** by 1.69 kcal/mol.

Scheme 4

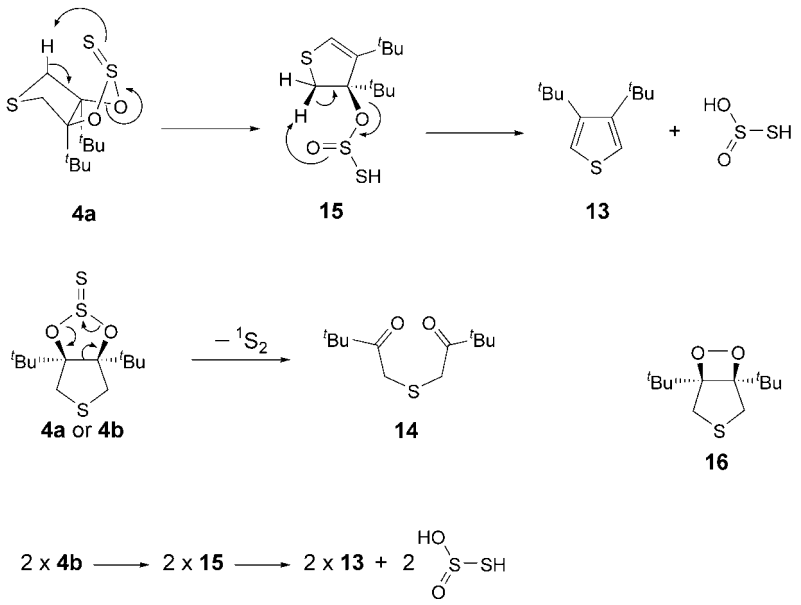

Thionosulfite **4a** is susceptible to alkaline hydrolysis. Thus, **4a** was hydrolyzed to the diol **5** in 93% yield in the presence of $NaHCO_3$ in a 1:1 mixture of H_2O and THF, whereas it remained unchanged in the absence of $NaHCO_3$ for several days.

Next, the reactivity of the thiosulfinyl group toward oxidants was examined. Oxidation of **4a** with an equimolar amount of dimethyldioxirane (DMD) gave **17a** in 91% yield, and oxidation of **4b** gave **17b** in 94% yield (*Scheme 5*). The structure of **17a** was determined by X-ray crystallographic analysis (*Fig. 11*), while the structure of **17b** was determined on the basis of its spectroscopic properties. The crystal data of **17a** are summarized in the *Exper. Part*.

Oxidation of **4a** with 1.1 mol-equiv. of '*m*-chloroperbenzoic acid' (MCPBA) gave **17a** and **18b** in a ratio of 94:6; **17a** was isolated in 77% yield. The use of 3.3 mol-equiv. of MCPBA gave **18b** and **19b** in a ratio of 90:10. The structures of **18b** and **19b** were determined by comparison of their spectroscopic data with those of authentic samples prepared by oxidation of **7b** [13]. These results show that the thiosulfinyl group is more-resistant toward oxidation than the S-atom in the CH_2-S-CH_2 moiety of the thiolane.

The above results also show that the oxidation of both **4a** and **4b** takes place exclusively *anti* (*exo* side) to the sulfite ring, *i.e.*, *syn* to the bulky *t*-Bu groups, and that the resulting configuration of each is the same as that observed previously for the

Scheme 5

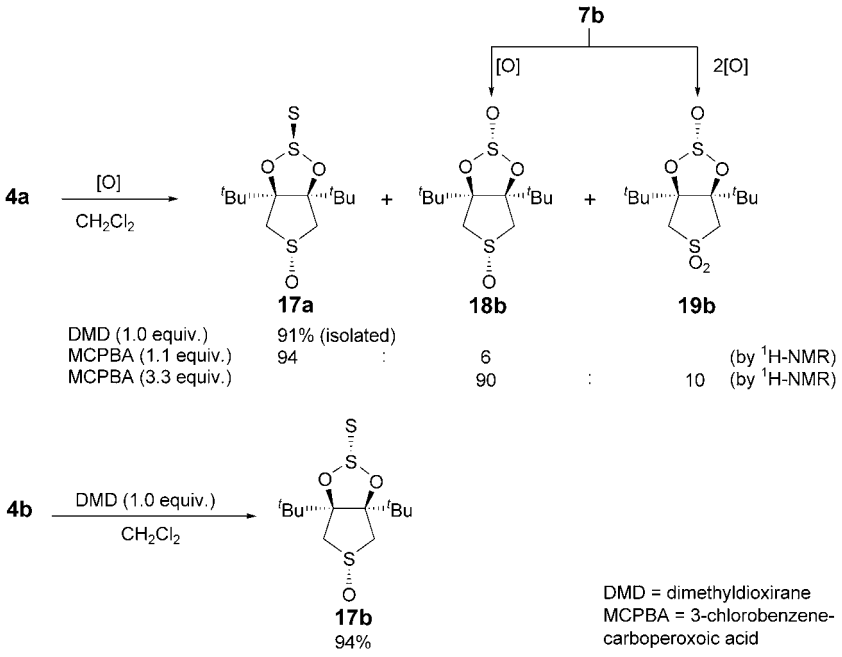

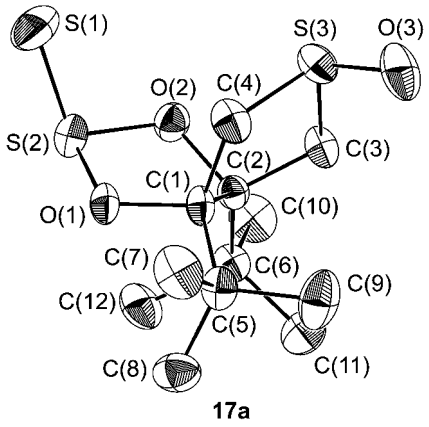

Fig. 11. *ORTEP Representation of the molecular structure of* **17a**. Relevant bond lengths [Å], bond angles [°], and dihedral angles [°]: S(1)–S(2), 1.8928(11); S(2)–O(1), 1.644(2); S(2)–O(2), 1.656(2); S(3)–O(3), 1.489(2); S(1)–S(2)–O(1), 111.08(7); S(1)–S(2)–O(2), 107.48(7); O(1)–S(2)–O(2), 97.73(8); O(1)–S(1)–S(2)–O(2), 43.47(14); C(3)–C(2)–C(1)–C(4), 37.3(2); C(5)–C(1)–C(2)–C(6), 43.1(2).

oxidation of **7a** and **7b** [13]. This would be best rationalized by steric hindrance: analysis of the molecular models based on X-ray crystallographic analyses of **4a** and **4b** suggests that the *exo* side is less hindered, in spite of the bulky *t*-Bu groups. The difference in the electron densities of the S-atom between *anti*- and *syn*-sides to the

sulfite ring would not be in accord with the results, because the DFT calculations predicted that there is no distinct difference for either **4a** and **4b** in the HOMO electron densities of the S-atoms between these two sides.

The above oxidation also converted the thiosulfinyl group to the sulfinyl group. We then investigated the oxidation of **17a** and **17b** with MCPBA, DMD, H_2O_2, and *t*-BuOCl to get more insight into the mechanism of this conversion (*Scheme 6*) [17]. The oxidations gave mixtures of **18a** and **18b**, with the ratios being dependent on the substrates and oxidants, as summarized in *Table 2*. Further oxidations of **18a** and **18b** to **19a** and **19b**, respectively, also took place (*Scheme 6* and *Entries 1–3* and *4* in *Table 2*). The structures of **18a** and **19a** were determined by comparison of the spectroscopic data

Scheme 6

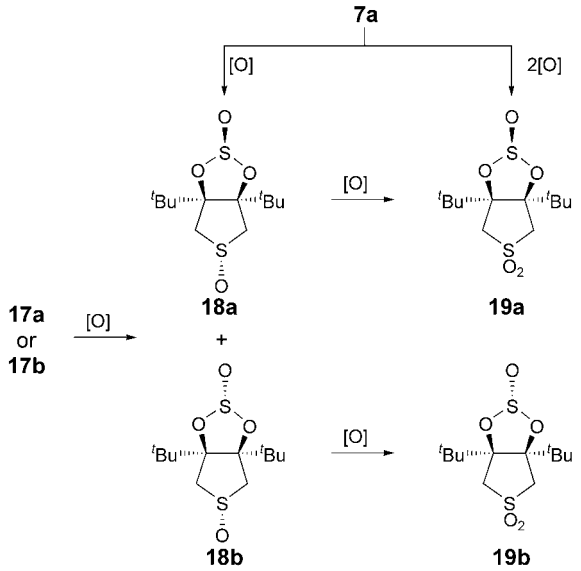

Table 2. *Oxidations of* **17a** *and* **17b**

Entry	Substrate	Oxidizing agent	Solvent	Product ratio[a])	
				17a/17b/18a/18b/19a/19b	**(18a + 19a)/(18b + 19b)**
1	**17a**	MCPBA[b])	CH_2Cl_2	8 : 0 : 14 : 66 : 0 : 12	15 : 85
2	**17b**	MCPBA[b])	CH_2Cl_2	0 : 8 : 34 : 37 : 9 : 12	47 : 53
3	**17a**	DMD[b])	CH_2Cl_2/Me_2CO	13 : 0 : 58 : 21 : 5 : 3	72 : 28
4	**17b**	DMD[b])	CH_2Cl_2/Me_2CO	0 : 15 : 50 : 23 : 7 : 5	67 : 33
5	**17a**	H_2O_2[c])	Me_2CO	46 : 0 : 4 : 50 : 0 : 0	7 : 93
6	**17b**	H_2O_2[c])	Me_2CO	0 : 59 : 16 : 25 : 0 : 0	39 : 61
7	**17a**	*t*BuOCl[d])	$CHCl_3$/THF	8 : 0 : 74 : 18 : 0 : 0	80 : 20
8	**17b**	*t*BuOCl[d])	$CHCl_3$/THF	10 : 3 : 71 : 16 : 0 : 0	82 : 18

[a]) Determined by ^{1}H-NMR analysis. [b]) With 2.2 mol-equiv. at 0° for 3 h. [c]) With excess H_2O_2 (30% soln.) at r.t. for 15 h. [d]) With 2.2 mol-equiv. at −50° for 15 min, then without cooling for 6 h.

with those of authentic samples prepared by oxidation of **7a** [13]. Note that 2 mol-equiv. of the oxidants are required for the conversion of **17** to **18**. This conversion shows a poor stereoselectivity (see the ratio (**18a** + **19a**)/(**18b** + **19b**) in *Table 2*). Thus, for *Entries 3*, *6*, and *7*, the configuration at the S-atom is mostly retained, for *Entries 1*, *4*, *5*, and *8*, the configuration at the S-atom is mostly inverted, and for *Entry 2*, no selectivity was observed. In addition, a separate experiment showed that, when the oxidation of **17a** with MCPBA was performed in the presence of 3,4-dimethylbuta-1,3-diene, compound **20**, which is the adduct of the diene with sulfur monoxide (SO), was obtained in 27% yield (*Scheme 7*) [18].

Scheme 7

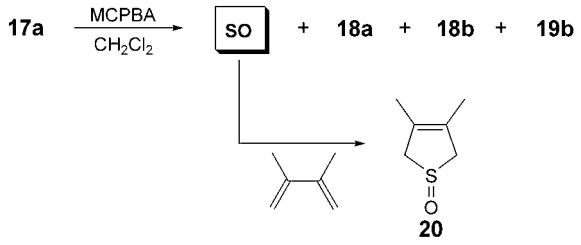

For the oxidation with MCPBA and DMD, three mechanisms should be taken into consideration, as illustrated in *Scheme 8* for **17a** as the substrate. In the case of Path *A*, initial oxidation takes place at the tetravalent S-atom from the *exo* face to produce a

Scheme 8

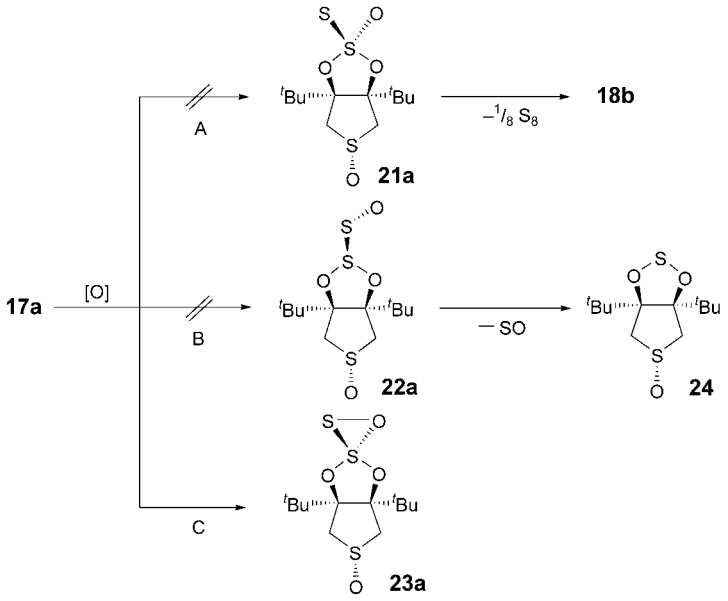

thionosulfate (**21a**). According to Path *B*, it takes place at the terminal S-atom to produce an intermediate (**22a**) with a new functional group (S=S=O). Route *C* is based on a three-membered-ring intermediate (**23a**), which corresponds to the epoxide formation from alkenes (see also *Scheme 9* below).

Scheme 9

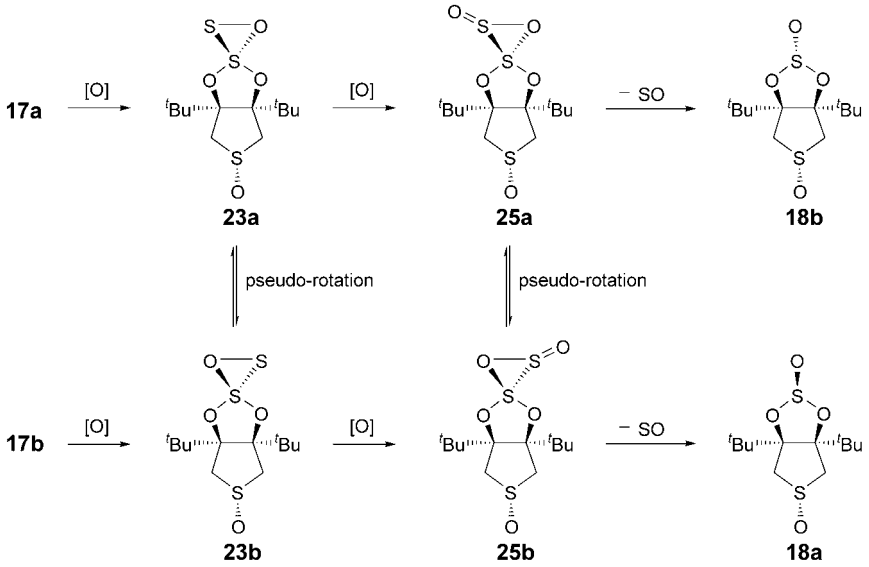

Mechanism *A* seems to be less probable because no sign of the formation of **21a** was observed, although **21a** might be more stable than **17a** and isolable (see the results of DFT calculations discussed later). In addition, if **18b** were formed through loss of an S-atom from **21a**, the reaction should take place with inversion at the S-center, and an equimolar amount of the oxidant should be enough to complete the oxidation to **18b**. However, no clean inversion of configuration was observed, and 2 mol-equiv. of the oxidants were required to complete the conversion. Furthermore, *Mulliken* population analysis predicted that the tetravalent S-atom of **17a**,**b** is considerably electron-deficient and, thus, hard to oxidize (*Fig. 12*).

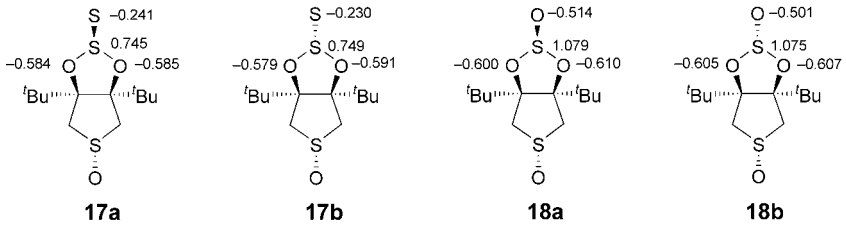

Fig. 12. Mulliken *population analyses of* **17a**,**b** *and* **18a**,**b** *at the B3LYP/6-31G* level*

For mechanism *B*, if **22a** once is formed, it might extrude SO to give a sulfoxylate (**24**). Although the mechanism is compatible with the formation of SO, which was

trapped by 3,4-dimethylbuta-1,3-diene, it does not rationalize the stereochemical outcome. If **24** exists as the intermediate, both oxidation of **17a** with MCPBA and that of **17b** should produce **18a** + **19a** and **18b** + **19b** in the same ratio. The same is true for the oxidation with DMD.

We will then consider mechanism *C* (*Scheme 9*). *Mulliken* population analysis[3]) predicted that the S=S bond of **17a**,**b** is less polarized than the S=O bond of **18a**,**b** (*Fig. 12*) [15]. Therefore, the three-membered-ring formation may take place to give **23**. Thus, oxidation of **17a** and **17b** gives the spiro compounds **23a** and **23b**, respectively. DFT Calculations predicted that these compounds are placed in the local energy minima, although they are thermodynamically less stable than **21a** and **22a** (*Fig. 13*) [15].

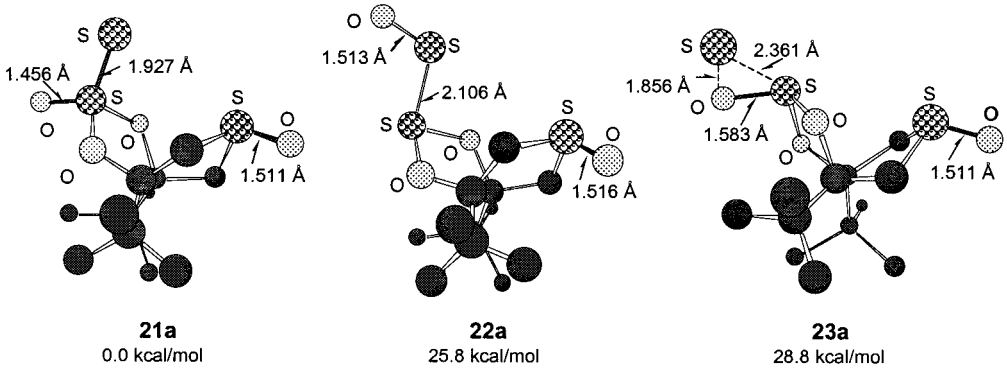

Fig. 13. *Predicted structures of the presumed intermediates* **21a**–**23a**

Compounds **23a** and **23b** might be interconvertible through pseudo-rotation[4]) [19]. The next oxidation takes place at the divalent S-atom to give **25a** from **23a**, and **25b** from **23b**, before the equilibrium is completed by pseudo-rotation. The interconversion between **25a** and **25b** by pseudo-rotation might also take place. Extrusion of SO from **25a** and **25b** gives **18b** and **18a**, respectively. Therefore, the ratio of **18a** to **18b**, *i.e.*, the ratio of (**18a** + **19a**) to (**18b** + **19b**), depends on the rate of oxidation of **23a** and **23b**, when there is no interconversion of **25a** and **25b**, *i.e.*, no pseudo-rotation. As a result, the ratio (**18a** + **19a**)/(**18b** + **19b**) becomes dependent on the substrates and oxidants. Thus, mechanism *C*, which initiates by formation of **23**, nicely accommodates the experimental observations and, thus, seems to be most likely, although we cannot rule out another mechanism, because the interconversion between **23a** and **23b**, whose trigonal-bipyramidal (TBP) structure is highly distorted, might have a high energy barrier[5]).

---

[4]) We thank Dr. *S. Sato* of Tsukuba University for discussions on the pseudo-rotation of the presumed intermediates.

[5]) A pseudo-rotation that takes place through the biradical intermediates formed by a hemolytic cleavage of the S–O bond of the three-membered ring would be least likely, since the hemolytic cleavage of, *e.g.*, **23a** should result in the formation of **21a**.

For the *t*-BuOCl oxidation, compounds **26a** and **26b** would form from **17a** and **17b**, respectively, through the formation of three-membered-ring intermediates (intermediates correspond to halonium ions for alkenes) by addition of Cl^+ to the S=S bond, followed by addition of H_2O (*Scheme 10*). Compounds **26a** and **26b** interconvert quickly by pseudo-rotation to give an equilibrium mixture. Hydrolysis of **26a** and **26b** will produce **18b** and **18a**, respectively. This rationalizes why the ratio of (**18a** + **19a**)/(**18b** + **19b**) is nearly equal for the oxidation of **17a** and **17b**.

Scheme 10

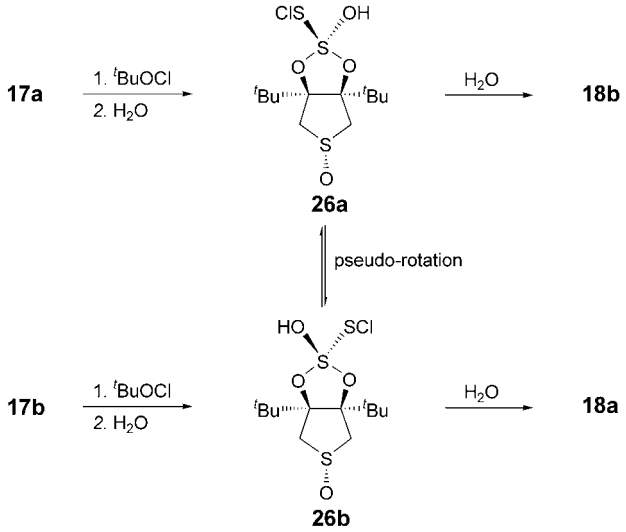

This work was supported by Grants-in-Aid for Scientific Research (Nos. 13029016 and 16350019) from the *Ministry of Education, Science, Culture and Technology*, Japan. We thank Prof. *A. Ishii* of Saitama University for fruitful discussions.

Experimental Part

1. *General*. Solvents were purified and dried in the usual manner. Column chromatography (CC) was performed on *Silica Gel 7734* (70–230 mesh; *Merck*) or *Silica Gel 60 N* (63–210 mesh; *Kanto*). Melting points (m.p.) were determined on a *Mel-Temp* capillary-tube apparatus and are uncorrected. UV Spectra were determined on a *JASCO V-560* spectrometer; λ_{max} (ε) in nm. IR Spectra were recorded on a *Perkin-Elmer System-2000* FT-IR spectrometer; in cm^{-1}. *Raman* spectra were taken on a *Perkin-Elmer System-2000* FT-*Raman* spectrophotometer; in cm^{-1}. ^1H- and ^{13}C-NMR Spectra were recorded on *Bruker ARX-400*, *Bruker AM-400*, or *Bruker AC-300P* spectrometers in $CDCl_3$ soln., with Me_4Si as internal standard; δ in ppm, J in Hz. Electron-impact mass spectra (EI-MS) were recorded on a *JEOL JMS-DX303* spectrometer operating at 70 eV; in *m*/*z*. Elemental analyses were performed by the Material and Life Science Research Center of Saitama University.

2. *Preparation of (3a*R,*6a*S*)-3a,6a-Di(*tert*-butyl)tetrahydrothieno[3,4-*d*][1,3,2]dioxathiole 2-Sulfide* (**4**). 2.1. *Reaction with 1,1′-Thiobis(1*H*-benzimidazole)* (**6**) *as Sulfur Transfer Agent*. 2.1.1. *Reaction at Room Temperature.* A mixture of cis-*3,4-di*(tert-*butyl*)*tetrahydrothiophene-3,4-diol* (**5**; 465 mg, 2.0 mmol) and **6** (2.34 g, 8.8 mmol) in MeCN (30 ml) was stirred for 72 h at r.t. The insoluble materials were removed by filtration, and the filtrate was evaporated. The resulting oily residue was stirred in hexane (*ca*. 30 ml), and the insoluble materials were removed again. The filtrate was evaporated to give a crude mixture of the *syn*- and *anti*-

isomers of **4**. The mixture was subjected to CC (SiO_2), and then to HPLC, to furnish 265 mg (45%) of **4a** (*syn*) and 59 mg (10%) of **4b** (*anti*).

Data of **4a**. Colorless plates. M.p. 110–111° (hexane). UV/VIS (hexane): 253 (2790), 324 (142). IR (KBr): 942, 817, 804, 791, 736, 693, 653 (S=S). *Raman* (neat): 816, 650 (S=S), 631, 594, 383, 287, 228. ^{1}H-NMR (400 MHz): 1.30 (*s*, 18 H); 3.41 (*d*, *J* = 13.4, 2 H); 3.90 (*d*, *J* = 13.4, 2 H). ^{13}C-NMR (100.6 MHz): 28.4 (br.); 35.5; 39.4; 111.1. EI-MS: 294 ($M^{+\bullet}$), 157. Anal. calc. for $C_{12}H_{22}O_2S_3$: C 48.94, H 7.53; found: C 49.05, H 7.57.

Data of **4b**. Colorless plates. M.p. 97–99° (hexane). UV/VIS (hexane): 245 (3060), 313 (203). IR (KBr): 967, 949, 810, 797, 735, 692, 670 (S=S). *Raman* (neat): 816, 666 (S=S), 623, 577, 330, 263. ^{1}H-NMR (400 MHz): 1.33 (*s*, 18 H); 3.13 (*d*, *J* = 14.1, 2 H); 3.42 (*d*, *J* = 14.1, 2 H). ^{13}C-NMR (100.6 MHz): 28.8 (br.); 38.6; 39.6; 107.0. EI-MS: 294 ($M^{+\bullet}$), 157. Anal. calc. for $C_{12}H_{22}O_2S_3$: C 48.94, H 7.53; found: C 49.16, H 7.57.

2.1.2. *Reaction at a Temperature of 40°*. Treatment of **5** (465 mg, 2 mmol) with **6** (2.13 g, 8 mmol) for 48 h at 40° in MeCN (30 ml) gave **4a** (236 mg, 40%) and **4b** (46 mg, 8%).

2.1.3. *Reaction in the Presence of 1,2,4-Triazole.* Treatment of **5** (58 mg, 0.25 mmol) with **6** (293 mg, 1.1 mmol) in the presence of 1,2,4-triazole (76 mg, 1.1 mmol) for 48 h at 40° in MeCN (4 ml) gave **4a** (37 mg, 50%) and **4b** (8 mg, 11%).

2.2. *Reaction with 1,1′-Thiobis(1*H*-1,2,4-triazole*) (**8**) *as Sulfur Transfer Agent*. Treatment of **5** (23 mg, 0.1 mmol) with **8** (74 mg, 0.4 mmol) for 50 h at r.t. in MeCN (2 ml) gave **4a** (4 mg, 14%) and **4b** (2 mg, 6%).

3. *Thermolyses of Compounds* **4a** *and* **4b**. A soln. of **4a** (1 mg, 3 μmol) in [D_8]toluene (0.5 ml) was heated at 120° for 96 h in a sealed NMR tube. The reaction led to **4a**, **13**, and **14** in a ratio of 48 : 39 : 13. The products were identified by comparison of their NMR chemical shifts with those of authentic samples. Although the progress of the reaction was monitored by ^{1}H-NMR, the formation of **4b** by isomerization of **4a** was not observed during this period. Similarly, a soln. of **4b** (1 mg, 3 μmol) in [D_8]toluene was heated at 120° in a sealed NMR tube. The reaction produced **13** and **14** in a ratio of 6 : 94, with complete consumption of **4b** after heating for 24 h. Although the progress of the reaction was monitored by ^{1}H-NMR, the formation of **4a** by isomerization of **4b** was not observed during this period.

4. *Hydrolysis of Compound* **4a**. A mixture of **4a** (3.9 mg, 0.013 mmol) and $NaHCO_3$ (4.5 mg, 0.05 mmol) in THF/H_2O 1 : 1 (4 ml) was stirred at r.t. for 45 h. The resulting mixture was washed with H_2O, dried ($MgSO_4$), and evaporated. ^{1}H-NMR Analysis showed that the residue (3 mg) was only composed of **5** and **4a** in a ratio of 96 : 4, corresponding to yields of 93 and 4%, resp.

5. *Oxidation Reactions.* 5.1. *Oxidation of* **4a** *with Dimethyldioxirane* (DMD). A 52-mM acetone soln. of DMD (3.1 ml, 0.16 mmol) was added to a soln. of **4a** (52.7 mg, 0.17 mmol) in CH_2Cl_2 (5 ml) at 0°, and the resulting mixture was stirred for 1.5 h. The mixture was evaporated, and the residue was purified by CC (SiO_2) to furnish **17a** (48.2 mg, 91%). Colorless plates. M.p. 148–150° (CH_2Cl_2/hexane; dec.). UV/VIS (hexane): 254 (2400), 320 (208). IR (KBr): 1042, 961, 952, 818, 799, 722, 677, 661. ^{1}H-NMR (300 MHz): 1.30 (*s*, 18 H); 3.05 (*d*, *J* = 14.7, 2 H); 4.60 (*d*, *J* = 14.7, 2 H). ^{13}C-NMR (75 MHz): 26.2 (br.); 39.0; 59.1; 107.1. EI-MS: 310 ($M^{+\bullet}$), 174, 111. Anal. calc. for $C_{12}H_{22}O_3S_3$: C 46.42, H 7.14; found: C 46.62, H 7.17.

5.2. *Oxidation of* **4b** *with DMD*. A 66.4-mM acetone soln. of DMD (1.5 ml, 0.10 mmol) was added to a soln. of **4b** (31.2 mg, 0.10 mmol) in CH_2Cl_2 (1.5 ml) at 0°, and the resulting mixture was stirred for 1.5 h. The mixture was evaporated, and the residue was purified by CC (SiO_2) to furnish **17b** (29.2 mg, 94%). Colorless plates. M.p. 146–148° (CH_2Cl_2/hexane; dec). UV/VIS (MeCN): 242 (2691), 312 (46). IR (KBr): 1042 (S=O), 973, 726, 686, 670 (S=S). ^{1}H-NMR (400 MHz): 1.35 (*s*, 18 H); 3.13 (*d*, *J* = 15.0, 2 H); 4.02 (*d*, *J* = 15.0, 2 H). ^{13}C-NMR (100 MHz): 27.0 (br.); 38.4; 61.2; 103.2. EI-MS: 310 ($M^{+\bullet}$), 174, 111. Anal. calc. for $C_{12}H_{22}O_3S_3$: C 46.42, H 7.14; found: C 46.65, H 7.16.

5.3. *Oxidation of* **4a** *with 3-Chloroperbenzoic acid* (MCPBA). 5.3.1. *With 1.1 Equiv. of Oxidant.* A mixture of **4a** (42.6 mg, 0.14 mmol) and MCPBA (27.5 mg, 0.16 mmol) in CH_2Cl_2 (3 ml) was stirred at −13° for 1 h. The resulting mixture was washed with H_2O, dried ($MgSO_4$), and evaporated. ^{1}H-NMR Analysis showed that the residue was composed of **17a** and **18b** in a ratio of 94 : 6. Crystallization from hexane/CH_2Cl_2 afforded syn,anti-*(3a*R,*6a*S*)-3a,6a-di(*tert*-butyl)tetrahydrothieno[3,4-*d*][1,3,2]dioxathiole 5-Oxide 2-Sulfide* (**17a**; 33.4 mg, 77%).

5.3.2. *With 3.3 Equiv. of Oxidant*. To a soln. of **4a** (35.8 mg, 0.12 mmol) in CH_2Cl_2 (3.5 ml) was added MCPBA (69.2 mg, 0.40 mmol) at 0°. The mixture was warmed to r.t. and stirred for 17 h. Then, the mixture was worked up as described above to afford a solid residue, which, according to ^{1}H-NMR analysis, was composed of **18b** and **19b** in a ratio of 90 : 10. The spectroscopic data of **18b** and **19b** agreed with those of authentic samples obtained by oxidation of **7b** [13].

5.4. *Oxidation of* syn,anti-*(3a*R,*6a*S*)-3a,6a-Di(*tert*-butyl)tetrahydrothieno[3,4-*d*][1,3,2]dioxathiole 5-Oxide 2-Sulfide* (**17a**). 5.4.1. *With MCPBA as Oxidant.* A mixture of **17a** (5.1 mg, 0.016 mmol) and MCPBA (6.0 mg, 0.035 mmol) in CH_2Cl_2 (1.5 ml) was stirred at 0° for 3 h. The resulting mixture was washed with H_2O, dried

($MgSO_4$), and evaporated. ^{1}H-NMR Analysis of the residue (5.5 mg) indicated **17a**, **18a**, **18b**, and **19b** in a ratio of 8:14:66:12. The spectroscopic data of **18a** agreed with those of an authentic sample obtained by oxidation of **7a** [13].

5.4.2. *With DMD as Oxidant.* A soln. of **17a** (12.2 mg, 0.039 mmol) in CH_2Cl_2 (1 ml) and a 51-mM acetone soln. of DMD (1.7 ml, 0.087 mmol) were combined at 0° and stirred for 3 h. The resulting mixture was evaporated. ^{1}H-NMR Analysis of the residue indicated **17a**, **18a**, **18b**, **19a**, and **19b** in a ratio of 13:58:21:5:3. The spectroscopic data of **19a** agreed with those of an authentic sample obtained by oxidation of **7a** [13].

5.4.3. *With H_2O_2 as Oxidant.* A mixture of **17a** (7.6 mg, 0.024 mmol) and an aq. 30% soln. of H_2O_2 (15.0 mg, 0.13 mmol) was stirred at 0° in acetone (2.0 ml), and then at r.t. for 15 h. ^{1}H-NMR Analysis of the crude product showed that the residue was composed of **17a**, **18a**, and **18b** in a ratio of 46:4:50.

5.4.4. *With* t-*BuOCl as Oxidant.* An 88-mM soln. of *t*-BuOCl in $CHCl_3$ (0.9 ml, 0.079 mmol) was added to a soln. of **17a** (11 mg, 0.035 mmol) in a binary mixture of $CHCl_3$ (0.6 ml) and THF (0.5 ml) at −50°. The mixture was stirred for 15 min, and then treated with ice-cold H_2O (2.5 ml). The resulting mixture was stirred without cooling for 6 h, diluted with CH_2Cl_2, washed with H_2O, dried ($MgSO_4$), and evaporated. ^{1}H-NMR Analysis of the residue (9.5 mg) indicated **17a**, **18a**, and **18b** in a ratio of 8:74:18.

5.5. *Oxidation of* anti,anti-*(3a*R,*6a*S*)-3a,6a-Di(*tert-*butyl)tetrahydrothieno[3,4-*d*][1,3,2]dioxathiole 5-Oxide 2-Sulfide* (**17b**). 5.5.1. *With MCPBA as Oxidant.* A mixture of **17b** (6.3 mg, 0.020 mmol) and MCPBA (7.6 mg, 0.044 mmol) in CH_2Cl_2 (1.5 ml) was stirred at 0° for 3 h. The resulting mixture was washed with H_2O, dried ($MgSO_4$), and evaporated. ^{1}H-NMR Analysis of the residue (6.5 mg) indicated **17b**, **18a**, **18b**, **19a**, and **19b** in a ratio of 8:34:37:9:12.

5.5.2. *With DMD as Oxidant.* A soln. of **17b** (5.8 mg, 0.018 mmol) in CH_2Cl_2 (1 ml) and a 66-mM acetone soln. of DMD (0.6 ml, 0.040 mmol) were combined at 0° and stirred for 3 h. The resulting mixture was evaporated. ^{1}H-NMR Analysis of the residue indicated **17b**, **18a**, **18b**, **19a**, and **19b** in a ratio of 15:50:23:7:5.

5.5.3. *With H_2O_2 as Oxidant.* A mixture of **17b** (12.7 mg, 0.040 mmol) and an aq. 30% soln. of H_2O_2 (25.0 mg, 0.22 mmol) was stirred at 0° in acetone (2.0 ml), and then at r.t. for 15 h. ^{1}H-NMR Analysis of the crude product indicated **17b**, **18a**, and **18b** in a ratio of 59:16:25.

5.5.4. *With* t-*BuOCl as Oxidant.* An 88-mM soln. of *t*-BuOCl in $CHCl_3$ (0.3 ml, 0.026 mmol) was added to a soln. of **17b** (3.6 mg, 0.012 mmol) in a mixture of $CHCl_3$ (0.5 ml) and THF (0.3 ml) at −50°. The mixture was stirred for 15 min, and then treated with ice-cold H_2O (2.5 ml). The resulting mixture was stirred without external cooling for 3 h, diluted with CH_2Cl_2, washed with H_2O, dried ($MgSO_4$), and evaporated. ^{1}H-NMR Analysis of the residue (3.5 mg) indicated **17a**, **17b**, **18a**, and **18b** in a ratio of 10:3:71:16.

6. *Trapping of Sulfur Monoxide.* A soln. of MCPBA (20.7 mg, 0.12 mmol) in CH_2Cl_2 (2.0 ml), and a soln. of the trapping agent 2,3-dimethylbuta-1,3-diene (0.045 ml, 0.4 mmol) in CH_2Cl_2 (3.0 ml) were added separately and slowly to a stirred soln. of **17a** (12.4 mg, 0.040 mmol) in CH_2Cl_2 (3.0 ml) at r.t. The mixture was stirred for 24 h and then evaporated. The residue was purified by CC (SiO_2; CH_2Cl_2/Et_2O 1:1) to afford a mixture (12.7 mg) composed of **17a**, **18a**, and **18b** in a ratio of 34:3:63. Further elution of the column (MeOH) gave an oily mixture (1.3 mg), which was purified by GPC (gel-permeation chromatography) [18] to afford **20** (0.9 mg, 27%).

7. *X-Ray Crystal Structures of* **4a**, **4b**, *and* **17a**. Crystal data were recorded on a *Mac Science DIP-3000* diffractometer equipped with a graphite monochromator. Oscillation and *Weissenberg* photographs were recorded on the imaging plates of the diffractometer with MoK_α radiation ($\lambda = 0.71073$ Å), and data reduction was performed with the MAC DENZO program system. The cell parameters were determined and refined with MAC DENZO for all observed reflections. The structures were solved by direct methods using SIR97 [20], and refined with full-matrix least-squares (SHELXL-97) methods [21] using all independent reflections. Absorption corrections for **4b** and **17a** were made by a multi-scan method (SORTAV) [22]. The non-H-atoms were refined anisotropically. The data are summarized in *Table 3*.

Crystallographic data for the structural analysis have been deposited with the *Cambridge Crystallographic Data Centre* as supplementary publication numbers CCDC-218636 (**4a**), -218637 (**4b**), and -218638 (**17a**). Copies of the data can be obtained, free of charge, from the CCDC, 12 Union Road, Cambridge CB2 1EZ, UK (fax: +44-1223-336033; e-mail: data_request@ccdc.cam.ac.uk; internet: http://www.ccdc.cam.ac.uk/data_request/cif).

Table 3. *Crystal Data of* **4a**, **4b**, *and* **17a**

	4a	**4b**	**17a**
Chemical formula	$C_{12}H_{22}O_2S_3$	$C_{12}H_{22}O_2S_3$	$C_{12}H_{22}O_3S_3$
Formula weight	294.50	294.50	310.51
Crystal shape	Cube	Cube	Cube
Crystal size [mm]	$0.20 \times 0.14 \times 0.14$	$0.20 \times 0.20 \times 0.16$	$0.32 \times 0.26 \times 0.14$
Crystal system	Monoclinic	Monoclinic	Orthorhombic
Space group	$P2_1/c$	$P2_1/c$	$P2_12_12_1$
a [Å]	8.660(1)	8.820(1)	8.622(1)
b [Å]	13.241(1)	8.425(1)	13.806(1)
c [Å]	13.140(1)	19.442(1)	24.820(1)
β [°]	109.381(2)	90.198(2)	
V [Å^3]	1424.16(12)	1444.70(13)	2954.5(2)
Z	4	4	8
D_{calc} (Mg m^{-3})	1.374	1.354	1.396
No. of measured refl.	3241	3043	3511
No. of independent refl.	3103	2861	3106
No. of observed refl. ($I > 2\sigma(I)$)	2500	2267	2357
No. of parameters	242	242	251
$R1$	0.034	0.061	0.046
$wR2$	0.084	0.178	0.123
Goodness-of-fit	1.033	1.069	0.984
T (K)	153	153	153
Δp_{max}	0.41	1.11	0.47
Δp_{min}	− 0.37	− 1.17	− 0.57

REFERENCES

[1] G. W. Kutney, K. Turnbull, *Chem. Rev.* **1982**, *82*, 333.

[2] R. L. Kuczkowski, E. B. Wilson Jr., *J. Am. Chem. Soc.* **1963**, *85*, 2028; R. L. Kuczkowski, *J. Am. Chem. Soc.* **1963**, *85*, 3047; R. L. Kuczkowski, *J. Am. Chem. Soc.* **1964**, *86*, 3617.

[3] a) Q. E. Thompson, M. M. Crutchfield, M. W. Dietrich, *J. Org. Chem.* **1965**, *30*, 2696; b) G. K. Abdullaev, I. A. Mamedov, M. M. Mamedov, *Azerb. Khim. Zh.* **1973**, *5–6*, 43; c) K. Miaskiewicz, R. Steudel, *J. Chem. Soc.*, *Dalton Trans.* **1991**, 2395; d) R. Steudel, Y. Drozdova, K. Miaskiewicz, R. H. Hertwig, W. Koch, *J. Am. Chem. Soc.* **1997**, *119*, 1990.

[4] a) D. N. Harpp, K. Steliou, C. J. Cheer, *J. Chem. Soc.*, *Chem. Commun.* **1980**, 825; b) J. P. Snyder, N. Nevins, S. L. Tardif, D. N. Harpp, *J. Am. Chem. Soc.* **1997**, *119*, 12685; c) E. Zysman-Colman, C. B. Abrams, D. N. Harpp, *J. Org. Chem.* **2003**, *68*, 7059.

[5] F. H. Allen, O. Kennard, D. G. Watson, L. Brammer, A. G. Orpen, R. Taylor, *J. Chem. Soc.*, *Perkin Trans. 2* **1987**, S1.

[6] S. C. Abrahams, *Acta Crystallogr.* **1955**, *8*, 661.

[7] F. Iwasaki, *Acta Crystallogr.*, *Sect. B* **1979**, *35*, 2099; C. Tamura, K. Aiba, S. Sato, T. Hata, S. Morimura, T. Yoshioka, *Acta Crystallogr.*, *Sect. B* **1977**, *33*, 3918.

[8] F. Rebiere, O. Samuel, L. Ricard, H. B. Kagan, *J. Org. Chem.* **1991**, *56*, 5991.

[9] J. Nakayama, S. Yamaoka, M. Hoshino, *Tetrahedron Lett.* **1988**, *29*, 1161; J. Nakayama, R. Hasemi, K. Yoshimura, Y. Sugihara, S. Yamaoka, *J. Org. Chem.* **1998**, *63*, 4912.

[10] D. N. Harpp, K. Steliou, T. H. Chan, *J. Am. Chem. Soc.* **1978**, *100*, 1222.

[11] S. Tanaka, Y. Sugihara, A. Sakamoto, A. Ishii, J. Nakayama, *J. Am. Chem. Soc.* **2003**, *125*, 9024.

[12] G. Mitchell, in 'Comprehensive Heterocyclic Chemistry II', Ed. R. C. Storr, Pergamon Press, Oxford, 1996, Vol. 4, Chapt. 4.15.

[13] S. Tanaka, Y. Sugihara, A. Sakamoto, A. Ishii, J. Nakayama, *Heteroat. Chem.* **2003**, *14*, 587.

[14] T. Benincori, E. Brenna, F. Sannicolò, L. Trimarco, P. Antognazza, E. Cesarotti, F. Demartin, T. Pilati, G. Zotti, *J. Organomet. Chem.* **1997**, *529*, 445.

[15] M. J. Frisch, G. W. Trucks, H. B. Schlegel, G. E. Scuseria, M. A. Robb, J. R. Cheeseman, V. G. Zakrzewski, J. A. Montgomery, R. E. Stratmann, J. C. Burant, S. Dapprich, J. M. Millam, A. D. Daniels, K. N. Kudin, M. C. Strain, O. Farkas, J. Tomasi, V. Barone, M. Cossi, R. Cammi, B. Mennucci, C. Pomelli, C. Adamo, S. Clifford, J. Ochterski, G. A. Petersson, P. Y. Ayala, Q. Cui, K. Morokuma, D. K. Malick, A. D. Rabuck, K. Raghavachari, J. B. Foresman, J. Cioslowski, J. V. Ortiz, A. G. Baboul, B. B. Stefanov, G. Liu, A. Liashenko, P. Piskorz, I. Komaromi, R. Gomperts, R. L. Martin, D. J. Fox, T. Keith, M. A. Al-Laham, C. Y. Peng, A. Nanayakkara, C. Gonzalez, M. Challacombe, P. M. W. Gill, B. Johnson, W. Chen, M. W. Wong, J. L. Andres, C. Gonzalez, M. Head-Gordon, E. S. Replogle, J. A. Pople, *Gaussian, Inc.*, Pittsburgh, PA, USA, 1998.

[16] C. H. Green, D. G. Hellier, *J. Chem. Soc., Perkin Trans. 2* **1972**, 458; C. H. Green, D. G. Hellier, *J. Chem. Soc., Perkin Trans. 2* **1973**, 243; J. G. Pritchard, P. C. Lauterbur, *J. Am. Chem. Soc.* **1961**, *83*, 2105; C. H. Green, D. G. Hellier, *J. Chem. Soc., Perkin Trans. 2* **1975**, 190; G. W. Buchanan, D. G. Hellier, *Can. J. Chem.* **1976**, *54*, 1428.

[17] C. R. Johnson, D. McCants Jr., *J. Am. Chem. Soc.* **1965**, *87*, 1109; G. Barbieri, M. Cinquini, S. Colonna, F. Montanari, *J. Chem. Soc. C* **1968**, 659; W. O. Siegl, C. R. Johnson, *J. Org. Chem.* **1970**, *35*, 3657; E. Block, E. J. Corey, R. E. Penn, T. L. Renken, P. F. Sherwin, *J. Am. Chem. Soc.* **1976**, *98*, 5715; I. Jalsovszky, F. Ruff, M. Kajtár-Peredy, A. Kucsman, *Synthesis* **1990**, 1037; D. V. Deubel, *J. Org. Chem.* **2001**, *66*, 2686; T. Patonay, W. Adam, A. Lévai, P. Kövér, M. Németh, E.-M. Peters, K. Peters, *J. Org. Chem.* **2001**, *66*, 2775.

[18] I. A. Abu-Yousef, D. N. Harpp, *J. Org. Chem.* **1997**, *62*, 8366; S. L. Tardif, A. Z. Rys, C. B. Abrams, I. A. Abu-Yousef, P. B. F. Lesté-Lasserre, E. K. V. Schultz, D. N. Harpp, *Tetrahedron* **1997**, *53*, 12225.

[19] R. S. Berry, *J. Chem. Phys.* **1960**, *32*, 933; S. Oae, M. Yokoyama, M. Kise, N. Furukawa, *Tetrahedron Lett.* **1968**, 4131; P. Gillespie, P. Hoffman, H. Klusacek, D. Marquarding, S. Pfohl, F. Ramirez, E. A. Tsolis, I. Ugi, *Angew. Chem., Int. Ed.* **1971**, *10*, 687; S. Oae, T. Kawai, N. Furukawa, F. Iwasaki, *J. Chem. Soc., Perkin Trans. 2* **1987**, 405; N. Furukawa, T. Shibutani, H. Fujihara, *Tetrahedron Lett.* **1987**, 5845.

[20] A. Altomare, M. C. Burla, M. Camalli, G. L. Cascarano, C. Giacovazzo, A. Guagliardi, A. G. G. Moliterni, G. Polidori, R. Spagna, *J. Appl. Crystallogr.* **1999**, *32*, 115.

[21] G. M. Sheldrick, SHELXL 97, Program for the Refinement of Crystal Structures, 1997.

[22] R. H. Blessing, *Acta Crystallogr., Sect. A* **1995**, *51*, 33.

Received January 18, 2005